JOURNAL OF GUIDANCE, CONTROL, AND DYNAMICS
Vol. 32, No. 4, July–August 2009

Proportional Navigation Miss Distance in the Presence of Bounded Inputs

Shaul Gutman* and Orly Goldan Ben-Aharon*
Technion—Israel Institute of Technology, 32000 Haifa, Israel

DOI: 10.2514/1.41713

This paper studies the guaranteed miss distance in case a missile is guided by proportional navigation, in which the guidance system is subject to bounded target maneuvers and bounded noise. It extends the results to the case in which the miss distance is the norm of a vector. This enables us to consider the usual miss distance due to target maneuvers combined by several bounded disturbances that act upon the guidance system. This novel approach is valid even in the case in which no statistical information is available. It replaces the stochastic approach by a deterministic approach and the root-mean-square miss by the worst (guaranteed) miss.

I. Introduction

PROPORTIONAL navigation (PN) is a well-known guidance strategy with more than half a century of history [1–3]. One of the most important issues in guidance is the miss distance due to a bounded maneuvering target. Over the years, researchers have developed the adjoint method as the primary approach to study the PN performances against maneuvering targets. In particular, a step target maneuver received much attention (see [3]). Mathematics has shown that at certain instances before termination, initiating the step maneuver is beneficial to the evasive target. On the other hand, if the target initiates its step maneuver a long time (in terms of the number of time constants) before termination, the miss distance vanishes. It is evident that a rational target will not settle for less than its best. Thus, the worst target maneuver problem becomes important. This problem for linear guidance was first addressed in [4] using optimal control. However, the solution in [4] is not in a general closed form. In [3], based on the adjoint method, the reader can find a nice interpretation of [4]. In [5], a more general solution is reported. Yet, the solution is not in a form suitable for numerical calculation.

Recently [6], a closed-form solution has been obtained as a special case of differential games. This solution uses Simulink as a simple numerical tool. Because optimal control is well known for a wide range of readers, we present a detailed solution to the optimal evasive maneuver based on a direct optimal control. Using a direct optimal control enables us to extend the results of [6] to the general vector zero-effort miss. Likewise, the paper deals, for the first time, with the adjoint approach to worst miss distance due to bounded inputs. This extends the previous adjoint approach to constant inputs [3]. The results are further extended to the case in which the miss distance is the norm of a vector rather than a scalar as in the two-dimensional motion. However, in the present paper, we will not extend the results to a three-dimensional motion. Rather, in addition to target maneuvers in the plane, the case is considered in which several bounded disturbances such as target maneuvers, gust, and noise act upon the guidance system. According to a classical approach, using shaping filters [3], target maneuvers are modeled as a stochastic input. Because noise is considered stochastic, one has a stochastic guidance loop, and the miss distance is measured in terms of root mean square (rms).

The present paper takes a novel route. In particular, both the target maneuver and the noise are modeled as arbitrary but bounded functions. This approach enables us to replace the rms miss by the worst miss. Moreover, one does not need any statistical assumptions or information on either the noise or the target except their bounds. On one hand, this approach is somewhat conservative with respect to the noise, but on the other hand, because miss distance is developed very close to termination, the noise may carry slow signals for a short time interval so that the real miss is larger than is expected from the stochastic approach. It is important to note that along with the stochastic approach to state estimation and control, some interesting literature on the so-called set-membership description of uncertainty has evolved (see [7–10] for early publications and [11–13] for more recent publications). We differ, however, from those papers in that we focus on the control part, whereas [7–13] are concerned more with the estimation part (with the exception of [9]). As far as numeric calculations, detailed block diagrams directly suitable for Simulink are presented.

The paper is organized as follows. Section II describes PN in a planar motion. In Sec. II, we develop the worst vector miss distance using optimal control and apply it to PN. In Sec. III, we do the same using the adjoint method. Section IV extends the results to the case in which the target is not ideal: that is, it has a nonunit transfer function. In Sec. V, we unify the notion of miss distance to include both target maneuver miss and noise miss. Section VI illustrates the results using a thrust vector control (TVC) example, and in Sec. VII, we present conclusions.

II. Proportional Navigation

Consider a nominal collision course (Fig. 1) in which two objects, a missile M and a target T, move in a plane in straight lines and with constant speeds toward a collision point C. The two objects maneuver in the neighborhood of this collision course, in which the missile's objective is to minimize the miss distance, whereas the target tends to maximize it.

We assume that along the line of sight (LOS), the range R satisfies the nominal relation:

$$R = V_c(t_f - t) \triangleq V_c\theta$$

where θ is the time-to-go, and the constant V_c is the closing speed. We further assume that for miss distance calculation, the perturbations are normal to the LOS. Letting $\Delta y = y_T - y_M := x_1$, we obtain the following linear model:

$$\dot{\mathbf{x}} = \mathbf{A}\mathbf{x} + \mathbf{B}u_c + \mathbf{C}v \tag{1}$$

where $\mathbf{x} = [x_1 \quad x_2 \quad \mathbf{z}']'$, $\dot{x}_1 = x_2$, $\mathbf{x} \in \mathbb{R}^{n+2}$, $\mathbf{z} \in \mathbb{R}^n$ is the missile state vector (normal to LOS), $\mathbf{A} \in \mathbb{R}^{(n+2)\times(n+2)}$, $\mathbf{B} \in \mathbb{R}^{(n+2)\times 1}$, $\mathbf{C} \in \mathbb{R}^{(n+2)\times 1}$, and

Received 20 October 2008; revision received 11 March 2009; accepted for publication 25 March 2009.

*Department of Mechanical Engineering.

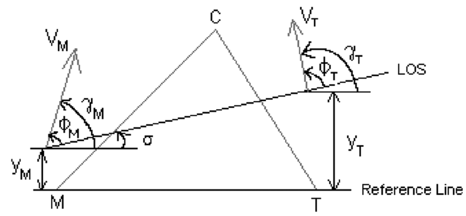

Fig. 1 Collision triangle and perturbations.

$$\mathbf{A} = \begin{bmatrix} 0 & 1 & 0 \\ 0 & 0 & -\hat{\mathbf{c}} \\ 0 & 0 & \hat{\mathbf{A}} \end{bmatrix} \qquad \mathbf{B} = \begin{bmatrix} 0 \\ -\hat{d} \\ \hat{\mathbf{b}} \end{bmatrix} \qquad \mathbf{C} = \begin{bmatrix} 0 \\ 1 \\ 0 \end{bmatrix} \tag{2}$$

where $\hat{\mathbf{A}} \in \mathbb{R}^{n\times n}$, $\hat{\mathbf{b}} \in \mathbb{R}^{n\times 1}$, $\hat{\mathbf{c}} \in \mathbb{R}^{1\times n}$, $\hat{d} \in \mathbb{R}^1$, $G_M := \{\hat{\mathbf{A}}, \hat{\mathbf{b}}, \hat{\mathbf{c}}, \hat{d}\}$ is the missile realization, with $G_M(s) = \hat{\mathbf{c}}(s\mathbf{I} - \hat{\mathbf{A}})^{-1}\hat{\mathbf{b}} + \hat{d}$ as its (lateral) transfer function, and the target is ideal. These equations can be described by a block diagram as in Fig. 2. Here, u_c and v are the acceleration command variables of the missile and the target, respectively, perpendicular to LOS.

PN is a guidance law in which the command acceleration u_c is proportional to the LOS rate:

$$u_c = N'(\theta)V_c\dot{\sigma} \tag{3}$$

where $N'(\theta)$ is the navigation gain, possibly a function of time-to-go. In the state space,

$$\sigma = \frac{x_1}{V_c\theta} \Rightarrow \theta^2 V_c\dot{\sigma} = x_1 + \theta\dot{x}_1, \qquad u_c = \frac{N'(\theta)}{\theta^2}(x_1 + \theta x_2) \tag{4}$$

Applying PN to the block diagram in Fig. 2, we obtain the closed-loop guidance block diagram described by Fig. 3a. In state space, the closed-loop proportional navigation becomes

$$\dot{\mathbf{x}} = \begin{bmatrix} 0 & 1 & \mathbf{0}_{1\times n} \\ -\frac{N'(\theta)}{\theta^2}\hat{d} & -\frac{N'(\theta)}{\theta}\hat{d} & -\hat{\mathbf{c}} \\ \frac{N'(\theta)}{\theta^2}\hat{\mathbf{b}} & \frac{N'(\theta)}{\theta}\hat{\mathbf{b}} & \hat{\mathbf{A}} \end{bmatrix}\mathbf{x} + \begin{bmatrix} 0 \\ 1 \\ \mathbf{0}_{n\times 1} \end{bmatrix} v \tag{5}$$

Going back to Fig. 3a, we can eliminate the noncausal differentiator in case $N'(\theta) = N'$ is *constant*, using block manipulations. In particular, Fig. 3a implies $x_2 = \int v\mathrm{d}t - \int u\mathrm{d}t$. Defining $\tilde{x}_2 = \int v\mathrm{d}t$, one has the transformation $\tilde{x}_2 = x_2 + \int u\mathrm{d}t$, and Fig. 3c follows. As a result, one has the following state equations:

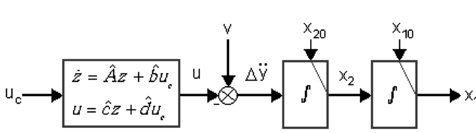

Fig. 2 Open-loop block diagram.

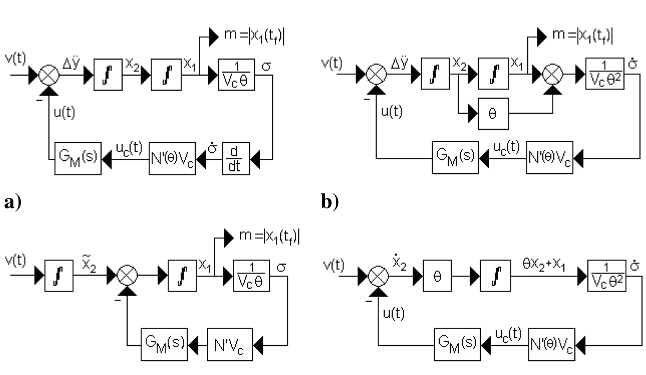

Fig. 3 PN diagrams: a) noncausal, B) causal, C) modified noncausal, and d) modified causal.

$$\dot{\mathbf{x}} = \begin{bmatrix} -\frac{N'}{\theta}\hat{d} & 1 & -\hat{\mathbf{c}} \\ 0 & 0 & \mathbf{0}_{1\times n} \\ \frac{N'}{\theta}\hat{\mathbf{b}} & \mathbf{0}_{1\times n} & \hat{\mathbf{A}} \end{bmatrix}\mathbf{x} + \begin{bmatrix} 0 \\ 1 \\ \mathbf{0}_{n\times 1} \end{bmatrix} v \tag{6}$$

where now $\mathbf{x} = [\,x_1 \quad \tilde{x}_2 \quad \mathbf{z}'\,]'$. Yet, another causal block diagram is shown in Fig. 3d.

With the preceding dynamics, we associate the miss distance $|x_1(t_f)|$ as the cost:

$$J = |\mathbf{D}x(t_f)|$$

where

$$\mathbf{D} = [\,1 \quad 0 \quad \mathbf{0}_{1\times n}\,]$$

That is,

$$\mathrm{Max}_{\,v} J = |\mathbf{D}x(t_f)| \quad \text{subject to dynamics Eq. (6)} \tag{7}$$

This problem was solved in [5] as a special case of a differential game (by nulling one player). In the next section, we present a direct optimal control approach. In particular, we are concerned with some basic issues of the preceding PN:

1) Given $|v(t)| \le \rho_v$, what is the worst target maneuver $v(t)$, with respect to the miss distance?

2) What is the guaranteed miss distance?

III. Worst Miss Distance

Consider the terminal cost optimal control

$$\max_{\mathbf{v}} J = \|\mathbf{D}\mathbf{x}(t_f)\| \tag{8}$$

$$\text{subject to } \dot{\mathbf{x}} = \mathbf{A}(t)\mathbf{x} + \mathbf{C}\mathbf{v} \tag{9}$$

$$\mathbf{v}'\mathbf{S}\mathbf{v} \le 1 \tag{10}$$

where $\mathbf{x} \in \mathbb{R}^{n+2}$, $\mathbf{v} \in \mathbb{R}^m$, $\mathbf{A}(t) \in \mathbb{R}^{(n+2)\times(n+2)}$ is a continuous time-varying matrix, $\mathbf{D} \in \mathbb{R}^{\ell\times(n+2)}$ and $\mathbf{C} \in \mathbb{R}^{(n+2)\times m}$ are constant matrices, and $\mathbf{S} \in \mathbb{R}^{m\times m}$ is a constant symmetric and positive definite matrix. Here, and in what follows, $\|\cdot\|$ is the $\|\cdot\|_2$ norm. First, we transform the state variable x into the zero-effort-miss variable $\mathbf{y} \in \mathbb{R}^\ell$ as follows:

$$\mathbf{y} = \mathbf{D}\mathbf{\Phi}(t_f, t)\mathbf{x} \tag{11}$$

$$\dot{\mathbf{\Phi}}(t_f, t) = -\mathbf{\Phi}(t_f, t)\mathbf{A}(t), \qquad \mathbf{\Phi}(t_f, t_f) = \mathbf{I} \tag{12}$$

where $\mathbf{\Phi}(t_f, t)$ is the transition matrix of $\mathbf{A}(t)$. Define

$$\mathbf{Y}(t_f, t) = \mathbf{D}\mathbf{\Phi}(t_f, t)\mathbf{C} \tag{13}$$

Then, the optimal control formulation becomes

$$\max_{\mathbf{v}} J = \|\mathbf{y}(t_f)\| \tag{14}$$

$$\text{subject to } \dot{\mathbf{y}} = \mathbf{Y}(t_f, t)\mathbf{v} \tag{15}$$

$$\mathbf{v}'\mathbf{S}\mathbf{v} \le 1 \tag{16}$$

Define the Hamiltonian:

$$H = \boldsymbol{\lambda}(t)'\mathbf{Y}(t_f, t)\mathbf{v} \tag{17}$$

where the adjoint variable $\boldsymbol{\lambda}(t)$ satisfies

$$\dot{\boldsymbol{\lambda}}(t) = -\frac{\partial H}{\partial \mathbf{y}} = 0, \longrightarrow \boldsymbol{\lambda}(t) = \text{const} \tag{18}$$

The transversality condition

$$\boldsymbol{\lambda}'(t_f) = \nabla_y \|\mathbf{y}\|_{t_f} = \frac{\mathbf{y}'(t_f)}{\|\mathbf{y}(t_f)\|} \longrightarrow \boldsymbol{\lambda}(t) = \frac{\mathbf{y}(t_f)}{\|\mathbf{y}(t_f)\|} \tag{19}$$

The optimal control $\mathbf{v}^*$ is obtained by maximizing the Hamiltonian, as follows.

Define

$$\mathbf{S}^{-1} = \mathbf{M}'\mathbf{M} \tag{20}$$

and the transformation

$$\mathbf{v}_1 = \mathbf{M}'^{-1}\mathbf{v} \tag{21}$$

Then,

$$\max_{\mathbf{v}'\mathbf{S}\mathbf{v}\le 1} H = \max_{\mathbf{v}'\mathbf{S}\mathbf{v}\le 1} \boldsymbol{\lambda}'\mathbf{Y}\mathbf{v} = \max_{\|\mathbf{v}_1\|\le 1} \boldsymbol{\lambda}'\mathbf{Y}\mathbf{M}'\mathbf{v}_1 \tag{22}$$

$$\longrightarrow \mathbf{v}^* = \mathbf{M}'\frac{\mathbf{M}\mathbf{Y}'\boldsymbol{\lambda}}{\|\mathbf{M}\mathbf{Y}'\boldsymbol{\lambda}\|} = \mathbf{M}'\frac{\mathbf{M}\mathbf{Y}'\mathbf{y}(t_f)}{\|\mathbf{M}\mathbf{Y}'\mathbf{y}(t_f)\|} \tag{23}$$

Suppose first that y is a *scalar* ($\mathbf{D} \in \mathbb{R}^{n+2}$ and $\mathbf{Y} \in \mathbb{R}^m$) but $\mathbf{v} \in \mathbb{R}^m$ is a vector. Then,

$$\dot{y}^* = \mathbf{Y}\mathbf{v}^* = \mathbf{Y}\mathbf{M}'\frac{\mathbf{M}\mathbf{Y}'y(t_f)}{\|\mathbf{M}\mathbf{Y}'y(t_f)\|} = \text{sgn}[y(t_f)]\|\mathbf{M}\mathbf{Y}'\|$$

Using the time-to-go variable θ,

$$\theta = t_f - t, \qquad d\theta = -dt$$

and using the fact that in PN guidance systems, $\mathbf{A} = \mathbf{A}(\theta)$, we have $\boldsymbol{\Phi} = \boldsymbol{\Phi}(\theta)$, $\mathbf{Y} = \mathbf{Y}(\theta)$, and

$$\frac{dy^*}{d\theta} = -\text{sgn}(y_0)\|\mathbf{M}\mathbf{Y}'(\theta)\|$$

where $y_0 = y(\theta = 0) = y(t = t_f)$.

Because of symmetry,

$$\frac{d|y^*|}{d\theta} = -\|\mathbf{M}\mathbf{Y}'(\theta)\| \tag{24}$$

Integrating, we obtain

$$|y^*| - |y_0| = -\int_0^\theta \|\mathbf{M}\mathbf{Y}'(\xi)\|\mathrm{d}\xi$$

or

$$|y_0| = |y^*| + \int_0^\theta \|\mathbf{M}\mathbf{Y}'(\xi)\|\mathrm{d}\xi \tag{25}$$

However, in the original optimization, $|y_0| = |y(t = t_f)|$ is the terminal cost, and the current state y^* of Eq. (25) is the initial state. Because we are interested in the miss distance due to target maneuvers, we assume $y^* = 0$ and define

$$m(\theta) := |y_0| = \int_0^\theta \|\mathbf{M}\mathbf{Y}'(\xi)\|\mathrm{d}\xi \tag{26}$$

The function $m(\theta)$ gives the worst miss distance θ s before termination. However, because the engagement duration can be forced by the target (for its benefit), we have to consider the possibility that the target maneuvers a long time before termination. It means that one has to maximize $m(\theta)$ with respect to θ. Because the integral of a nonnegative function is nondecreasing, we may increase the upper limit to infinity. Thus, the worst possible miss distance m due to target maneuvers becomes

$$m = \int_0^\infty \|\mathbf{Y}(\xi)\mathbf{M}'\|\mathrm{d}\xi \tag{27}$$

Does this integral converge? Can the target force an arbitrarily large miss distance? In a future publication [14], it will be shown that if $G_M(s)$ is strictly proper and asymptotically stable, $G_M(0) = 1$, and $N' \ge 2$, and the preceding infinite integral indeed converges. The optimal target maneuver becomes

$$\mathbf{v}^*(\theta) = \pm\mathbf{M}'\frac{\mathbf{M}\mathbf{Y}'(\theta)}{\|\mathbf{M}\mathbf{Y}'(\theta)\|} \tag{28}$$

The preceding result is valid for the case in which $\mathbf{v}$ is constrained by an ellipsoid. In case $\mathbf{v}$ is constrained by rectangle, we replace Eqs. (8–10), by

$$\max_{\mathbf{v}} J = \|\mathbf{D}\mathbf{x}(t_f)\| \qquad \text{subject to } \dot{\mathbf{x}} = \mathbf{A}(t)\mathbf{x} + \mathbf{C}\mathbf{v} \qquad |v_i(t)| \le \rho_i \tag{29}$$

If y is a scalar, it is easy to show that

$$m = \sum_i \rho_i \int_0^\infty |Y_i(\xi)|\mathrm{d}\xi \tag{30}$$

$$v_i^*(\theta) = \pm\rho_i \text{sgn}(Y_i(\theta)) \tag{31}$$

In our case, y and v are both scalars. In particular, $\mathbf{D} = [1 \quad 0 \quad 0]$, $\mathbf{C} = [0 \quad 1 \quad 0]'$, and $Y = \mathbf{D}\boldsymbol{\Phi}\mathbf{C} = \phi_{12}$. Thus, it is left to find $\phi_{12}(\theta)$. Using $\mathbf{D}\dot{\boldsymbol{\Phi}} = -\mathbf{D}\boldsymbol{\Phi}\mathbf{A}$ and $\Phi(t_f, t_f) = \mathbf{I}$, we obtain, in terms of θ, three differential equations in ϕ_{11}, ϕ_{12}, and $\boldsymbol{\phi}_{13}$, as follows:

$$\frac{d}{d\theta}[\phi_{11} \quad \phi_{12} \quad \boldsymbol{\phi}_{13}] = [\phi_{11} \quad \phi_{12} \quad \boldsymbol{\phi}_{13}]\mathbf{A} \tag{32}$$

where $\mathbf{A} = \mathbf{A}(\theta)$ is given in Eq. (5) and, for clarity, is explicitly recalled here:

$$\mathbf{A} = \begin{bmatrix} 0 & 1 & \mathbf{0}_{1\times n} \\ -\frac{N'(\theta)}{\theta^2}\hat{d} & -\frac{N'(\theta)}{\theta}\hat{d} & -\hat{\mathbf{c}} \\ \frac{N'(\theta)}{\theta^2}\hat{\mathbf{b}} & \frac{N'(\theta)}{\theta}\hat{\mathbf{b}} & \hat{\mathbf{A}} \end{bmatrix} \tag{33}$$

In particular, the three differential equations are

$$\begin{aligned} \frac{d\phi_{11}}{d\theta} &= -\frac{N'(\theta)\phi_{12}}{\theta^2}\hat{d} + \frac{N'(\theta)\boldsymbol{\phi}_{13}}{\theta^2}\hat{\mathbf{b}}, \qquad \phi_{11}(0) = 1 \\ \frac{d\phi_{12}}{d\theta} &= \phi_{11} - \frac{N'(\theta)\phi_{12}}{\theta}\hat{d} + \frac{N'(\theta)\boldsymbol{\phi}_{13}}{\theta}\hat{\mathbf{b}}, \qquad \phi_{12}(0) = 0 \\ \frac{d\boldsymbol{\phi}_{13}}{d\theta} &= -\phi_{12}\hat{\mathbf{c}} + \boldsymbol{\phi}_{13}\hat{\mathbf{A}}, \qquad \boldsymbol{\phi}_{13}(0) = 0 \end{aligned} \tag{34}$$

Observing the first two equations, one finds

$$\frac{d\phi_{12}}{d\theta} = \phi_{11} + \theta\frac{d\phi_{11}}{d\theta}$$

or

$$\frac{d\phi_{12}}{d\theta} = \frac{d}{d\theta}(\theta\phi_{11})$$

Direct integration with the initial conditions $\phi_{11}(0) = 1$ and $\phi_{12}(0) = 0$ yields

$$\phi_{12} = \theta\phi_{11}$$

Using the Laplace transform in the third equation,

$$\boldsymbol{\phi}_{13}(s) = -\hat{\mathbf{c}}(s\mathbf{I} - \hat{\mathbf{A}})^{-1}\phi_{12}(s)$$

Substituting in the first equation,

$$\frac{d\phi_{11}}{d\theta} = -\frac{N'(\theta)}{\theta^2} L^{-1}\{[\hat{\mathbf{c}}(s\mathbf{I} - \hat{\mathbf{A}})^{-1}\hat{\mathbf{b}} + \hat{d}]\phi_{12}(s)\}$$

Thus, Eqs. (34) reduce to

$$\phi_{12} = \theta\phi_{11}, \qquad \phi_{11}(0) = 1$$
$$\dot{\phi}_{11} = -\frac{N'(\theta)}{\theta^2}[L^{-1}\{G_M(s)\phi_{12}(s)\}] \tag{35}$$

and Eqs. (30) and (31) reduce to

$$m = \rho_v \int_0^\infty |\phi_{12}(\xi)|\mathrm{d}\xi \tag{36}$$

$$v^* = \pm\rho_v \mathrm{sgn}(\phi_{12}) \tag{37}$$

where $L^{-1}(\cdot)$ is the inverse Laplace transform with respect to θ, $G_M := \{\hat{\mathbf{A}}, \hat{\mathbf{b}}, \hat{\mathbf{c}}, \hat{d}\}$, and $G_M(s) = [\hat{\mathbf{c}}(s\mathbf{I} - \hat{\mathbf{A}})^{-1}\hat{\mathbf{b}} + \hat{d}]$. The preceding equations are best illustrated using the block diagram in Fig. 4. A typical function $m(\theta)$ is illustrated in Fig. 5.

Now we elaborate on the preceding results. As mentioned before, $\phi_{12} = \theta\phi_{11}$ implies $\dot{\phi}_{12} = \phi_{11} + \theta\dot{\phi}_{11}$. Thus, we can replace Fig. 4 by Fig. 6. It is interesting to recognize the feedback loop in Fig. 6 as the adjoint of Fig. 3b. Moreover, the preceding results are valid in the case $N' = N'(\theta)$. In case N' is *constant*, we may simplify the block diagram. Using Eq. (6) instead of Eq. (5), repeating the preceding calculations, we end up with the differential equations:

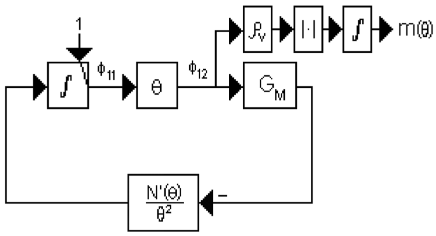

Fig. 4 Worst miss adjoint diagram.

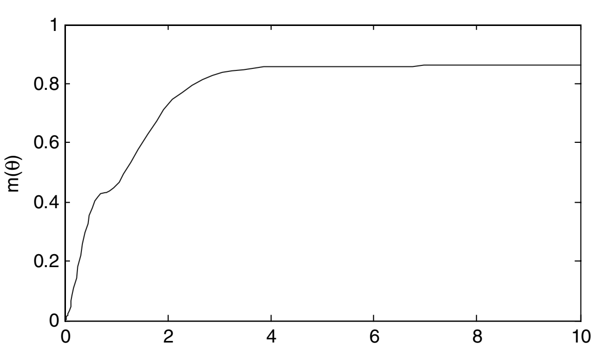

Fig. 5 Typical function $m(\theta)$.

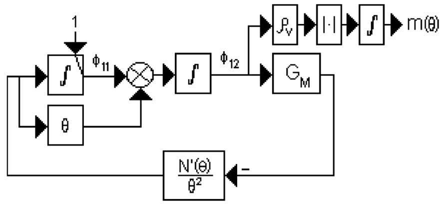

Fig. 6 Alternative worst miss adjoint diagram.

$$\dot{\phi}_{11} = -\frac{N'}{\theta}[L^{-1}\{G_M(s)\phi_{11}(s)\}], \qquad \dot{\phi}_{12} = \phi_{11}, \qquad \phi_{11}(0) = 1 \tag{38}$$

The block diagram description of these equations is depicted in Fig. 7. Clearly, this diagram is equivalent to the diagram in Fig. 4 for the case in which N' is constant.

Next, we wish to generalize the guaranteed miss distance (27) to a nonscalar y. To this end, recall that with respect to t,

$$\dot{\mathbf{y}}^* = \mathbf{Y}\mathbf{v}^* = \frac{\mathbf{Y}\mathbf{M}'\mathbf{M}\mathbf{Y}'\mathbf{y}(t_f)}{\|\mathbf{M}\mathbf{Y}'\mathbf{y}(t_f)\|}$$

Using the time-to-go variable θ and defining the constant unit vector (along an optimal path),

$$\boldsymbol{\zeta} = \frac{\mathbf{y}_0}{\|\mathbf{y}_0\|} = \frac{\mathbf{y}(\theta = 0)}{\|\mathbf{y}(\theta = 0)\|}$$

one has

$$\frac{d\mathbf{y}^*}{d\theta} = -\frac{\mathbf{Y}\mathbf{M}'\mathbf{M}\mathbf{Y}'\mathbf{y}_0/\|\mathbf{y}_0\|}{\|\mathbf{M}\mathbf{Y}'\mathbf{y}_0\|/\|\mathbf{y}_0\|} = -\frac{\mathbf{Y}\mathbf{M}'\mathbf{M}\mathbf{Y}'\boldsymbol{\zeta}}{\|\mathbf{M}\mathbf{Y}'\boldsymbol{\zeta}\|}$$

Multiplying from the left by the constant vector $\boldsymbol{\zeta}'$ yields

$$\boldsymbol{\zeta}'\frac{d\mathbf{y}^*}{d\theta} = -\|\mathbf{M}\mathbf{Y}'(\theta)\boldsymbol{\zeta}\|$$

Integrating,

$$\boldsymbol{\zeta}'(\mathbf{y} - \mathbf{y}_0) = -\int \|\mathbf{M}\mathbf{Y}'(\theta)\boldsymbol{\zeta}\|\mathrm{d}\theta$$

$$\boldsymbol{\zeta}'\mathbf{y} - \|\mathbf{y}_0\| = -\int \|\mathbf{M}\mathbf{Y}'(\theta)\boldsymbol{\zeta}\|\mathrm{d}\theta$$

$$\|\mathbf{y}_0\| = \boldsymbol{\zeta}'\mathbf{y} + \int \|\mathbf{M}\mathbf{Y}'(\theta)\boldsymbol{\zeta}\|\mathrm{d}\theta$$

Because $\boldsymbol{\zeta}$ is a unit vector, it follows that

$$\|\mathbf{y}_0\| \le \|\mathbf{y}\| + \int_0^\theta \|\mathbf{M}\mathbf{Y}'(\xi)\|\mathrm{d}\xi$$

Because we are interested here in the contribution of the target maneuver to the miss distance, we assume zero initial conditions, $\mathbf{y} = 0$, to obtain

$$\|\mathbf{y}_0\| \le \int_0^\theta \|\mathbf{M}\mathbf{Y}'(\xi)\|\mathrm{d}\xi$$

Finally, the worst miss distance becomes

$$m = \int_0^\infty \|\mathbf{Y}(\xi)\mathbf{M}'\|\mathrm{d}\xi \tag{39}$$

where $\mathbf{Y}(\xi)$ is a matrix function with appropriate dimensions.

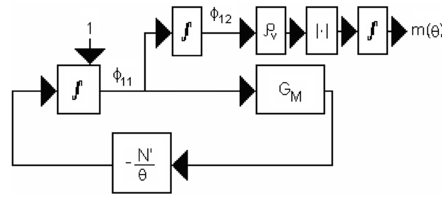

Fig. 7 Constant-N' worst miss adjoint diagram.

IV. Adjoint Analysis

The preceding analysis is based on a direct optimal control, whereas that of [6] is a special case of a differential game. As mentioned previously, the results are connected to the adjoint block diagram. This fact should not surprise the reader, as optimal control is based on the adjoint variable. In this section, we wish to apply the adjoint approach directly. Recall that the classical adjoint approach deals with step target maneuvers [3]. Here, we show that the extension to the worst bounded target maneuver is straightforward. Let $g(t,\tau)$ be the response of a linear system at time t to an impulse at time τ. Let $\tilde{g}(t_f-\tau, t_f-t)$ be the response of the adjoint system at $t_f-\tau$ to an impulse at t_f-t. Then, $\tilde{g}(t_f-\tau, t_f-t)=g(t,\tau)$ (see [15]). As a result, at time t_f, $\tilde{g}(t_f-\tau,0)=g(t_f,\tau)$. However, using convolution, we have the response

$$y(t_f)=\int_0^{t_f} g(t_f,\tau)v(\tau)\mathrm{d}\tau \tag{40}$$

Because $|v(t)|\le\rho_v$, it now follows that

$$\begin{aligned}|y(t_f)| &\le \rho_v\int_0^{t_f}|g(t_f,\tau)|\mathrm{d}\tau=\rho_v\int_0^{t_f}|\tilde{g}(t_f-\tau,0)|\mathrm{d}\tau\\ &=\rho_v\int_0^{t_f}|\tilde{g}(\xi,0)|\mathrm{d}\xi \triangleq \rho_v\int_0^{t_f}|\tilde{g}(\xi)|\mathrm{d}\xi\end{aligned} \tag{41}$$

where $\xi=t_f-\tau$ plays the role of θ. In short,

$$|y(t_f)|\le\rho_v\int_0^{t_f}|\tilde{g}(\xi)|\mathrm{d}\xi \tag{42}$$

Finally,

$$m=\rho_v\int_0^{\infty}|\tilde{g}(\xi)|\mathrm{d}\xi \tag{43}$$

To generalize this result to the multivariable case, define the matrix impulse response $\mathbf{G}(t,\tau)=[g_{ij}(t,\tau)]\in\mathbb{R}^{n\times n}$ and its adjoint matrix $\bar{\mathbf{G}}(t_f-\tau,t_f-t)$. As before, with the transformation $\mathbf{v}_1=\mathbf{M}'^{-1}\mathbf{v}$, we now have

$$m=\int_0^{\infty}\|\bar{\mathbf{G}}(\xi)\mathbf{M}'\|\mathrm{d}\xi \tag{44}$$

Comparing with Eq. (27), we recognize $\mathbf{Y}(\theta)=\mathbf{D}\Phi(\theta)\mathbf{C}$ as the matrix impulse response with respect to the adjoint variable θ.

V. Nonideal Target

So far, we have presented block diagrams for calculating the worst miss distance in case the target is ideal. Because targets are not ideal, we wish to study the effect of target dynamics on the miss distance. To this end, we modify Fig. 3a by adding a realization $\{\tilde{\mathbf{A}},\tilde{\mathbf{b}},\tilde{\mathbf{c}}\}$ to the target, with $G_T(s)=\tilde{\mathbf{c}}(s\mathbf{I}-\tilde{\mathbf{A}})^{-1}\tilde{\mathbf{b}}+\tilde{d}$ as a transfer function, and where v_c is the command target lateral acceleration (maneuver). The resulting PN block diagram is Fig. 8. As in Sec. II, we apply PN to obtain the closed-loop system:

$$\dot{\mathbf{x}}=\begin{bmatrix}0 & 1 & 0 & 0\\ -\frac{N'}{\theta^2}\hat{d} & -\frac{N'}{\theta}\hat{d} & -\hat{\mathbf{c}} & \tilde{\mathbf{c}}\\ \frac{N'}{\theta^2}\hat{\mathbf{b}} & \frac{N'}{\theta}\hat{\mathbf{b}} & \hat{\mathbf{A}} & 0\\ 0 & 0 & 0 & \tilde{\mathbf{A}}\end{bmatrix}\mathbf{x}+\begin{bmatrix}0\\ \tilde{d}\\ 0\\ \tilde{\mathbf{b}}\end{bmatrix}v_c \tag{45}$$

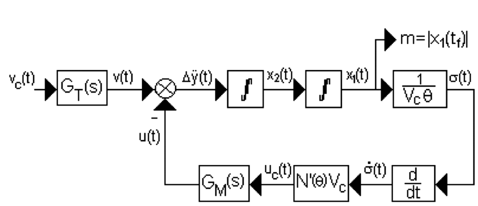

Fig. 8 PN with nonideal target.

Repeating the preceding adjoint approach or the optimal control version, one ends up with the adjoint block diagrams described in Figs. 9 and 10.

VI. Unified Miss

It is assumed that the reader of this section is familiar with the adjoint approach to noise-driven systems [3,16]. In particular, we call the attention of the reader to [3] (Figs. 7.15, 7.16). A comparison of Fig. 5 with [3] (Fig. 7.16) leads to a striking conclusion: namely, *the worst miss distance due to a target deterministic maneuver and the noise miss standard deviation have the same characteristics*. To study the implications of this conclusion, consider first a PN loop with two inputs, angular noise w and a maneuvering target v, as described by Fig. 11. It is assumed that the LOS angle σ is corrupted by white noise with power spectral density Φ_0 and zero mean and that the angular noise is processed through an estimator of the form $F(s)=s/a(s)$ to produce the estimated LOS rate $\hat{\dot{\sigma}}$. Note that the combination of noise followed by a differentiator in the PN loop magnifies the noise effect. Thus, the purpose of the estimator is to suppress the noise to prevent saturation as much as possible on one hand, but on the other hand, to avoid the insertion of slow dynamics into the guidance loop. Figure 12 describes the well-known adjoint loop (along with step and worst target maneuver miss), and Fig. 13 describes a simplification in case the gain N' is constant. These two figures reveal why the characteristics of the functions $m_{\text{opt}}(\theta)$ and $m_{\text{noise}}(\theta)$ look the same. However, because $m_{\text{opt}}(\theta)$ is the worst case and $m_{\text{noise}}(\theta)$ is rms, it is not natural to add them up. To unify all miss sources, it is suggested here to consider *bounded noise*. It means that

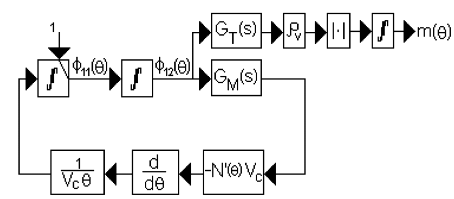

Fig. 9 Worst miss adjoint diagram for nonideal target.

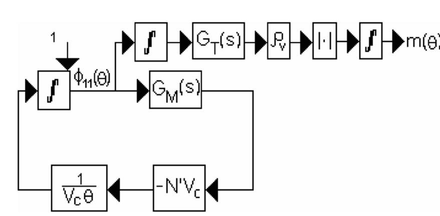

Fig. 10 Worst miss for nonideal target and constant N'.

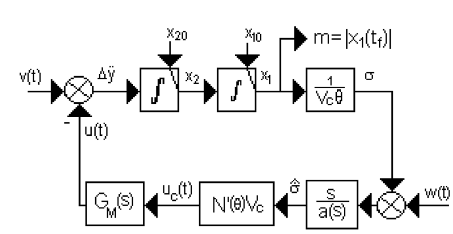

Fig. 11 PN with angular noise and target maneuver.

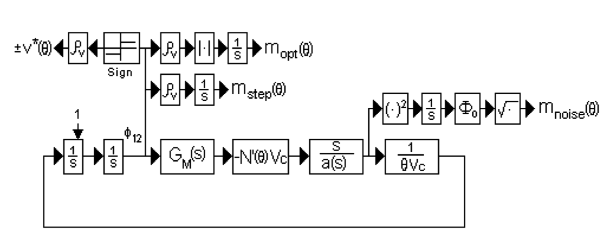

Fig. 12 PN adjoint for stochastic noise and target maneuver.

the noise is an *arbitrary but bounded* function with a known bound ρ_w. It includes noise of nonzero mean, nonstationary, any distribution, and nonergodic. This standpoint is a deterministic alternative to the stochastic approach, in which, in addition to the noise, the target too is stochastic [3]. In this paper, the estimator $F(s)$ mentioned previously is selected using either the stochastic approach or using the ellipsoidal calculus [7–13] as a guideline, and the worst miss distance due to bounded target maneuvers and bounded noise is calculated.

Let the missile dynamics be

$$G_M(s) \triangleq \begin{cases} \dot{\mathbf{z}} = \hat{\mathbf{A}}\mathbf{z} + \hat{\mathbf{b}}u_c \\ u = \hat{\mathbf{c}}\mathbf{z} + \hat{d}u_c \end{cases}$$

and the filter dynamics

$$F(s) \triangleq \begin{cases} \dot{z}_F = \hat{\mathbf{A}}_F\mathbf{z}_F + \hat{\mathbf{b}}_F(\sigma + w) \\ \hat{\sigma} = \hat{\mathbf{c}}_F\mathbf{z}_F \end{cases}$$

It is assumed that $F(s)$ is strictly proper and that it includes a free s. Define the state vector $\mathbf{x} = [x_1 \quad x_2 \quad \mathbf{z}' \quad \mathbf{z}_F']'$. Then the open-loop takes the form

$$\dot{\mathbf{x}} = \begin{bmatrix} 0 & 1 & 0 & 0 \\ 0 & 0 & -\hat{\mathbf{c}} & 0 \\ 0 & 0 & \hat{\mathbf{A}} & 0 \\ \hat{\mathbf{b}}_F/V_c\theta & 0 & 0 & \hat{\mathbf{A}}_F \end{bmatrix}\mathbf{x} + \begin{bmatrix} 0 \\ -\hat{d} \\ \hat{b} \\ 0 \end{bmatrix}u_c + \begin{bmatrix} 0 & 0 \\ 1 & 0 \\ 0 & 0 \\ 0 & \hat{b}_F \end{bmatrix}\begin{bmatrix} v \\ w \end{bmatrix}$$

The PN guidance law is

$$u_c = N'(\theta)V_c\hat{\sigma} = N'(\theta)V_c\hat{\mathbf{c}}_F\mathbf{z}_F$$

Thus, the closed-loop becomes

$$\dot{\mathbf{x}} = \begin{bmatrix} 0 & 1 & 0 & 0 \\ 0 & 0 & -\hat{\mathbf{c}} & -N'V_c\hat{\mathbf{c}}_F\hat{d} \\ \mathbf{0} & 0 & \hat{\mathbf{A}} & N'V_c\hat{\mathbf{c}}_F\hat{\mathbf{b}} \\ \hat{\mathbf{b}}_F/V_c\theta & 0 & 0 & \hat{\mathbf{A}}_F \end{bmatrix}\mathbf{x} + \begin{bmatrix} 0 & 0 \\ 1 & 0 \\ 0 & \mathbf{0} \\ 0 & \hat{\mathbf{b}}_F \end{bmatrix}\begin{bmatrix} v \\ w \end{bmatrix}$$

It is assumed that the target maneuver v and the noise w are arbitrary functions but are constrained either to an ellipsoid or to rectangle, according to Fig. 14.

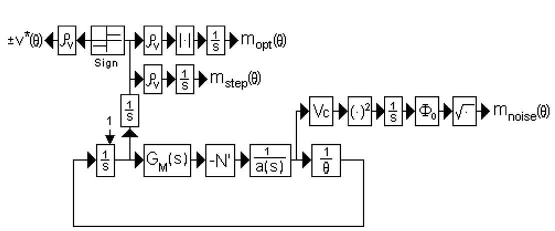

Fig. 13 PN adjoint for stochastic noise and target maneuver for constant N'.

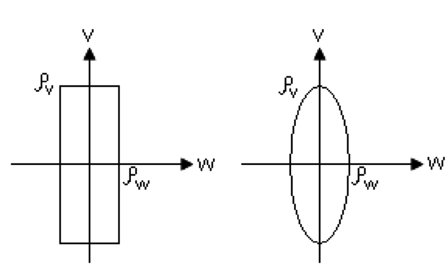

Fig. 14 Input-constrained set.

Define the zero-effort-miss variable

$$y = \mathbf{D\Phi}(\theta)\mathbf{x} \tag{46}$$

$$\frac{d\mathbf{\Phi}}{d\theta} = \mathbf{\Phi}(\theta)\mathbf{A}(\theta), \qquad \mathbf{\Phi}(0) = I \tag{47}$$

In particular,

$$\frac{d\phi_{11}}{d\theta} = \frac{1}{V_c\theta}\phi_{14}\hat{\mathbf{b}}_F, \qquad \phi_{11}(0) = 1, \qquad \frac{d\phi_{12}}{d\theta} = \phi_{11}$$

$$\phi_{12}(0) = 0, \qquad \frac{d\phi_{13}}{d\theta} = -\phi_{12}\hat{\mathbf{c}} + \phi_{13}\hat{A}, \qquad \phi_{13}(0) = 0$$

$$\frac{d\phi_{14}}{d\theta} = -N'(\theta)V_c\hat{\mathbf{c}}_F\hat{d}\phi_{12} + N'(\theta)V_c\hat{\mathbf{c}}_F\phi_{13}\hat{\mathbf{b}} + \phi_{14}\hat{\mathbf{A}}_F$$

$$\phi_{14}(0) = 0$$

It can be verified that

$$\frac{d\phi_{12}}{d\theta} = \phi_{11}, \qquad \phi_{13}(s) = -\hat{\mathbf{c}}(s\mathbf{I} - \hat{\mathbf{A}})^{-1}\phi_{12}(s)$$

$$\phi_{14}(s) = L\{N'(\theta)V_cL^{-1}[G_M(s)\phi_{12}(s)]\} \cdot \hat{\mathbf{c}}_F(s\mathbf{I} - \hat{\mathbf{A}}_F)^{-1}$$

Thus,

$$\frac{d\phi_{11}}{d\theta} = \frac{1}{\theta}L^{-1}\{L[N'(\theta)L^{-1}(G_M(s)\phi_{12}(s))] \cdot F(s)\}$$

To calculate the worst miss distance,

$$\mathbf{Y}(\theta) = \mathbf{D\Phi C} = \begin{bmatrix} \phi_{11} & \phi_{12} & \phi_{13} & \phi_{14} \end{bmatrix}\begin{bmatrix} 0 & 0 \\ 1 & 0 \\ 0 & \mathbf{0} \\ 0 & \hat{\mathbf{b}}_F \end{bmatrix}$$
$$= \begin{bmatrix} \phi_{12} & L^{-1}\{L[N'(\theta)V_cL^{-1}(G_M(s)\phi_{12}(s))] \cdot F(s)\} \end{bmatrix}$$

Thus,

$$\mathbf{S} = \begin{bmatrix} \rho_v^{-2} & 0 \\ 0 & \rho_w^{-2} \end{bmatrix}, \qquad \mathbf{M} = \begin{bmatrix} \rho_v & 0 \\ 0 & \rho_w \end{bmatrix}$$
$$\mathbf{MY}' = \begin{bmatrix} \rho_v\phi_{12} \\ \rho_wL^{-1}\{L[N'(\theta)V_cL^{-1}(G_M(s)\phi_{12}(s))] \cdot F(s)\} \end{bmatrix} \tag{48}$$

Finally, the total miss distance for the rectangle case is calculated with the aid of Eqs. (48) and (30) and described by Fig. 15. In case N' is constant, a simplification is possible according to Fig. 16.

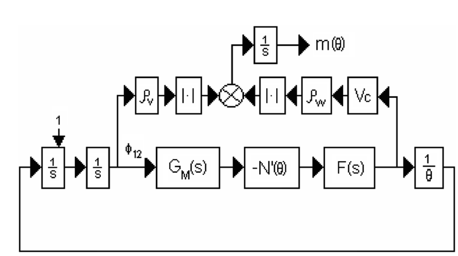

Fig. 15 Rectangle worst miss distance.

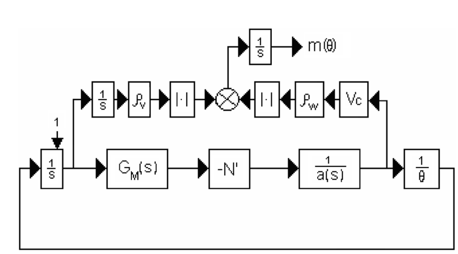

Fig. 16 Rectangle worst miss distance for constant N'.

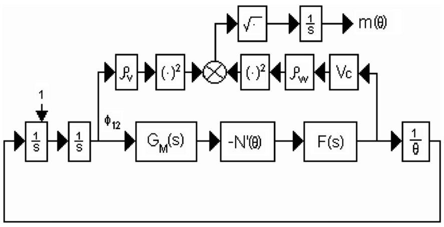

Fig. 17 Ellipsoid worst miss distance.

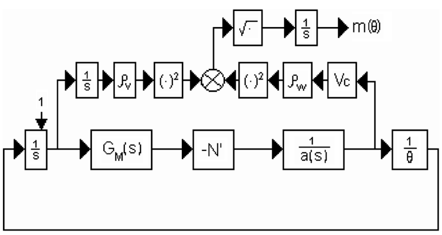

Fig. 18 Ellipsoid worst miss distance for constant N'.

Likewise, the total miss distance for the ellipsoid case is calculated with the aid of Eqs. (48) and (27) and described by Fig. 17. In case N' is constant, a simplification is possible according to Fig. 18.

VII. Thrust Vector Control Example

Consider a TVC missile as described in Fig. 19. Assume that angles α and δ are small. Further assume quasi stationarity: the missile speed has a small change during a step lateral response. Neglecting jet damping, the lateral equations of motion are

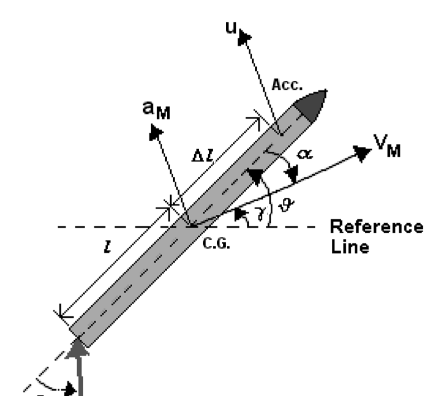

Fig. 19 TVC missile.

$$m \cdot V_M \cdot \dot{\gamma} = T \cdot (\delta + \alpha), \qquad \text{force} \perp \text{ to } V_M$$

$$I_y \cdot \ddot{\vartheta} = -T \cdot l \cdot \delta, \qquad \text{rotation}, \qquad \vartheta = \gamma + \alpha, \qquad \text{geometry} \tag{49}$$

where m is the missile mass, I_y is the missile lateral moment of inertia, V_M is the missile speed, T is the missile thrust, γ is the path angle (with respect to an inertial frame), α is the missile angle of attack, δ is the missile thrust deflection, and ϑ is the missile body orientation.

Define

$$\tau = \frac{m \cdot V_M}{T} \text{ s}, \qquad B = \frac{T \cdot l}{I_y} \text{ s}^{-1} \tag{50}$$

where l is the distance from the center of mass to the nozzle. Then,

$$\tau \cdot \dot{\gamma} = \delta + \alpha \qquad \ddot{\vartheta} = -B \cdot \delta \qquad \vartheta = \gamma + \alpha \tag{51}$$

and after some algebra,

$$\dot{\alpha} = -\frac{1}{\tau}\alpha + \dot{\vartheta} - \frac{1}{\tau}\delta \qquad \ddot{\vartheta} = -B \cdot \delta \qquad \dot{\gamma} = \dot{\vartheta} - \dot{\alpha} \tag{52}$$

This set of open-loop equations is suitable for a computer simulation. For control purposes, we measure the pitch rate $\dot{\vartheta}$ and the nose (accelerometer) lateral acceleration $V_M\dot{\gamma} + \Delta l \ddot{\vartheta}$, as the output. According to Fig. 20, the autopilot consists of a constant-pitch-rate feedback and a first-order lateral acceleration compensator. In this way, we control the nose rather than the c.g. lateral acceleration. Based on Fig. 20, the closed-loop transfer function $G_M(s)$ is

$$G_M(s) = \frac{K(s+z)((V_M - \tau B \Delta l)s^2 - (B\Delta l)s - BV_M)}{V_M(s+p)(Ts^2 + s - BK_{\dot{\vartheta}})(\tau s + 1) + K(s+z)((V_M - \tau B \Delta l)s^2 - (B\Delta l)s - BV_M)}$$

The reader can verify that the closed-loop transfer function is minimum phase if, and only if, $\Delta l \geq V_M/\tau B$.

As an illustration, consider a PN guidance system according to Fig. 11. Let the estimator (filter) $F(s)$ be a second-order fading-memory digital filter transformed into the continuous time:

$$F(s) = \frac{s}{a(s)} = \frac{(1-\beta)^2 s}{\beta^2 T_s^2 s^2 + 2\beta(1-\beta)T_s s + (1-\beta)^2}$$

We choose the data $\tau = 12$ s, $B = 200$ s^{-2}, $\Delta l = 1$ m, $K = -30$, $K_{\dot{\vartheta}} = -0.2$, $T = 0.02$ s, $p = 3$, $z = 6$, $N' = 3$, $V_M = 1800$ m/s, $V_c = 4000$ m/s, $\rho_v = 10$ m/s^2, $\rho_w = 0.0001$ rad, $T_s = 0.01$ s, and $\beta = 0.65$. For illustration, The numerical results are obtained with the aid of Simulink as follows. Figures 19 and 20 describe the adjoint runs for the rectangle and the ellipsoid cases, respectively. The corresponding forward-loop runs are displayed in Figs. 21 and 22. This is done with the aid of the worst target maneuver and the worst bounded noise that are calculated using the adjoint runs and are displayed in Figs. 23–28.

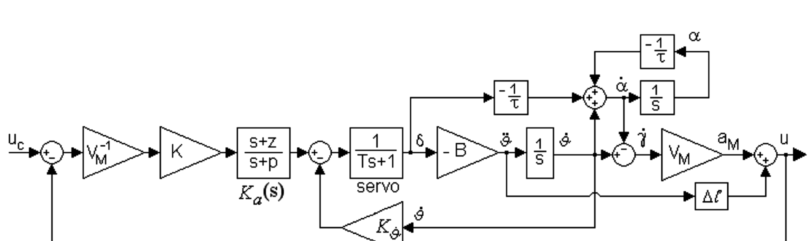

Fig. 20 TVC autopilot.

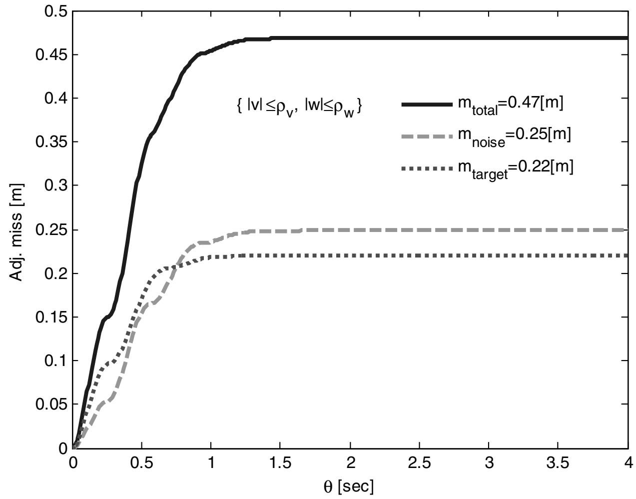

Fig. 21 Rectangle worst miss (Fig. 16).

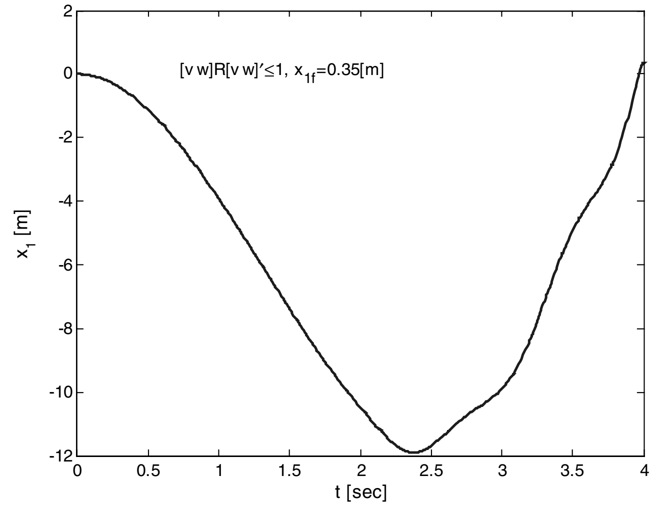

Fig. 24 Ellipsoid separation $x_1(t)$ (Fig. 11).

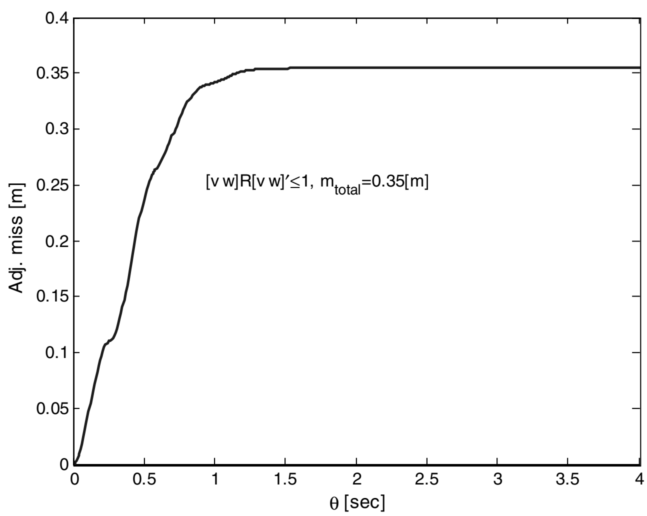

Fig. 22 Ellipsoid worst miss (Fig. 18).

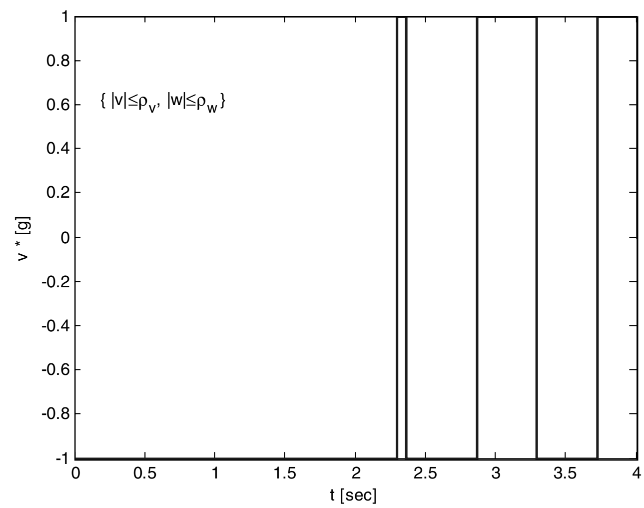

Fig. 25 Rectangle worst target maneuver.

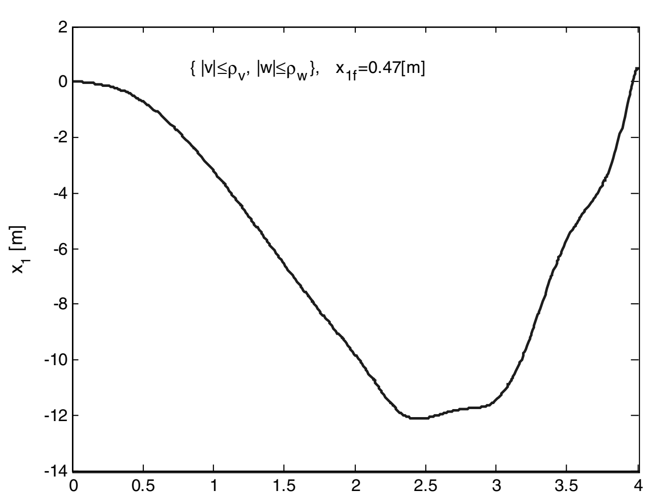

Fig. 23 Rectangle separation $x_1(t)$ (Fig. 11).

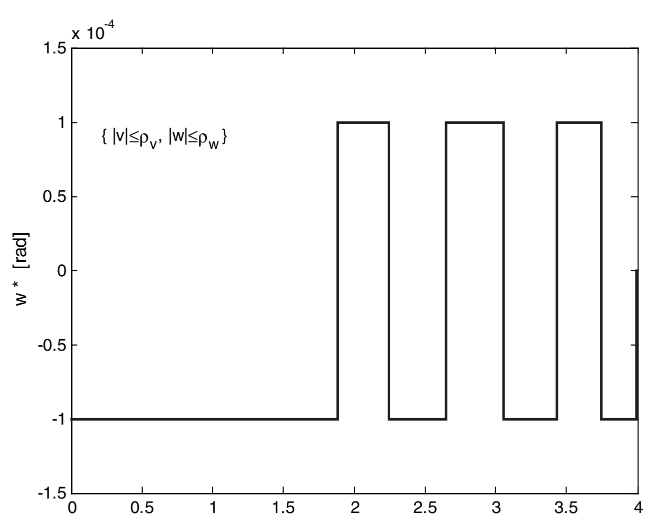

Fig. 26 Rectangle worst noise function.

VIII. Conclusions

In this paper, a novel approach to the worst miss distance in PN systems is presented. Both the target maneuver and the noise are arbitrary bounded functions having no statistical properties, such as zero mean, white or not, or ergodicity. This relaxation is a real advantage. A filter estimating the LOS rate is used to suppress the noise amplification due to a pure noise differentiation. Both the filter and the missile dynamics are taken into account in the worst miss

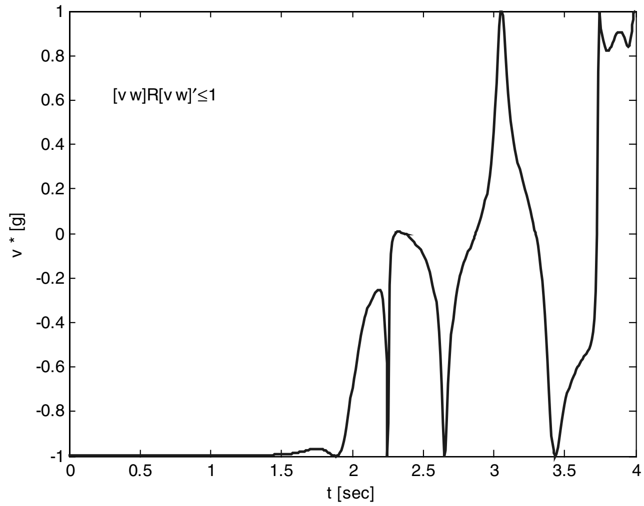

Fig. 27 Ellipsoid worst target maneuver.

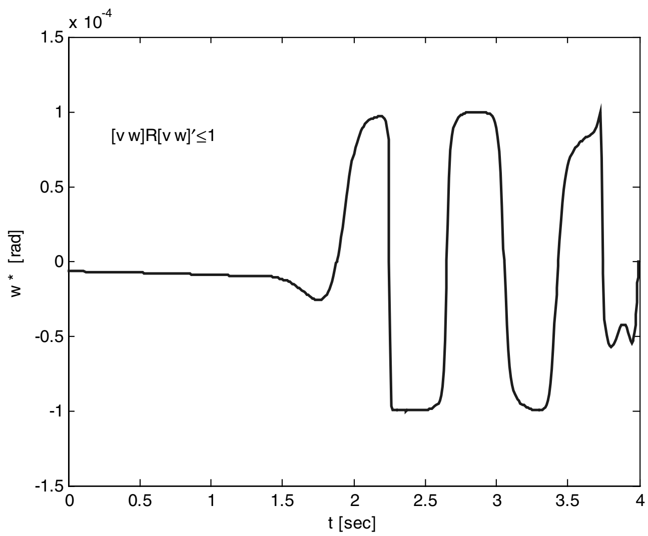

Fig. 28 Ellipsoid worst noise function.

calculation with respect to target maneuvers and noise. This calculation of the miss has the form of an adjoint loop and is simple for implementation. Note that although we are used to thinking of the noise as a high-frequency signal, the worst noise signal is not, as can be seen in Figs. 24 and 26. Comparing the miss due to white noise with that due to the worst bounded noise, we conclude that the former is smaller than the latter. Thus, bounded noise may be conservative, depending on the noise power. On the other hand, we have to take into account the possibility that a real noise may carry some low-frequency signals that may increase the noise miss. The mathematical reason for a such possible behavior lies in the fact that miss distance is developed only a short time before termination. Thus, for a short time interval, the noise may carry such low-frequency signals. This issue needs a further exploration and is left for future research. Finally, we mention that it is possible to extend the results of this paper to the three-dimensional motion. It is also left for a future investigation.

References

[1] Yuan, C. L., "Homing and Navigation Courses of Automatic Target-Seeking Devices," *Journal of Applied Physics*, Vol. 19, Dec. 1948, pp. 1122–1128.
doi:10.1063/1.1715028

[2] Fossier, M. W., "The Development of Radar Homing Missiles," *Journal of Guidance, Control, and Dynamics*, Vol. 7, Nov–Dec. 1984, pp. 641–651.
doi:10.2514/3.19908

[3] Zarchan, P., *Tactical and Strategic Missile Guidance*, 3rd ed., Progress in Astronautics and Aeronautics, AIAA, Vol. 176, Reston, VA, 1997.

[4] Shinar, J., and Stienberg, D., "Analysis of Optimal Evasive Maneuvers Based on a Linearized Two-Dimensional Model," *Journal of Aircraft*, Vol. 14, No. 8, 1977, pp. 795–802.
doi:10.2514/3.58855

[5] Shinar, J., and Gutman, S., "Three-Dimensional Optimal Pursuit and Evasion with Bounded Controls," *IEEE Transactions on Automatic Control*, Vol. 25, No. 3, June 1980, pp. 492–496.

[6] Gutman, S., *Applied Min-Max Approach to Missile Guidance and Control*, Vol. 209, Progress in Astronautics and Aeronautics, AIAA, Reston, VA, 2005.

[7] Witsenhausen, H. S., "Sets of Possible States of Linear Systems Given Perturbed Observations," *IEEE Transactions on Automatic Control*, Vol. 13, No. 5, 1968, pp. 556–558.
doi:10.1109/TAC.1968.1098995

[8] Schweppe, F. C., "Recursive State Estimation: Unknown But Bounded Errors and System Inputs," *IEEE Transactions on Automatic Control*, Vol. 13, No. 1, 1968, pp. 22–28.
doi:10.1109/TAC.1968.1098790

[9] Glover, J. D., and Schweppe, F. C., "Control of Linear Dynamic Systems with Set Constrained Disturbances," *IEEE Transactions on Automatic Control*, Vol. 16, No. 5, 1971, pp. 411–423.
doi:10.1109/TAC.1971.1099781

[10] Schweppe, F. C., *Uncertain Dynamic Systems*, Prentice–Hall, Upper Saddle River, NJ, 1973.

[11] Milanese, M., and Vicino, A., "Optimal Estimation Theory for Dynamic Systems with Set Membership Uncertainty: An Overview," *Automatica*, Vol. 27, No. 6, 1991, pp. 997–1009.
doi:10.1016/0005-1098(91)90134-N

[12] Maksarov, D. G., and Norton, J. P., "State Bounding with Ellipsoidal Set Description of the Uncertainty," *International Journal of Control*, Vol. 65, No. 5, 1996, pp. 847–866.
doi:10.1080/00207179608921725

[13] Kurzhanskii, A. B., and Vályi, I., *Ellipsoidal Calculus for Estimation and Control*, Birkhauser, Boston, 1997.

[14] Gutman, S., and Goldan Ben Aharon, O., "Stability and Miss Distance in Proportional Navigation," *IEEE Transactions on Aerospace and Electronic Systems* (submitted for publication).

[15] Kailath, T., *Linear Systems*, Prentice–Hall, Upper Saddle River, NJ, 1980.

[16] Laning, J. H., and Battin, R. H., *Random Processes in Automatic Control*, McGraw–Hill, New York, 1956.